Solvent effects on nuclear shieldings and spin–spin couplings of hydrogen selenide

Per-Olof Åstrand and Kurt V. Mikkelsen
Chemistry Laboratory III, H. C. Ørsted Institute, University of Copenhagen, Universitetsparken 5, DK-2100 Copenhagen Ø, Denmark

Poul Jørgensen
Department of Chemistry, University of Aarhus, Langelandsgade 140, DK-8000 Århus C, Denmark

Kenneth Ruud[a)]
Department of Physics and Measurement Technology, Linköping University, S-58183 Linköping, Sweden

Trygve Helgaker
Department of Chemistry, University of Oslo, Box 1033, Blindern, N-0315 Oslo, Norway

(Received 25 August 1997; accepted 6 November 1997)

Solvent effects on the nuclear shielding and indirect spin–spin coupling constants of H_2Se have been calculated by modeling the surroundings as a continuous dielectric medium. Gauge-origin independence of the nuclear shieldings is ensured by using London atomic orbitals in combination with linear response theory. We present the linear response function of a solvated molecule subject to triplet perturbations and use a new implementation of this theory to evaluate the Fermi-contact and spin–dipole contributions to the indirect spin–spin coupling constants. We present high-level calculations of the nuclear shielding and indirect spin–spin coupling constants of H_2Se in vacuum and different solvents. Our results represent the first *ab initio* calculations of the spin–spin coupling constants in H_2Se as well as the first investigation of medium effects on these properties. It is demonstrated that the solvent shifts of the spin–spin couplings are caused by a polarization of the molecular electronic structure as well as by changes in the geometry upon solvation. © *1998 American Institute of Physics.* [S0021-9606(98)03706-4]

I. INTRODUCTION

The NMR spectrum of a molecule is a sensitive probe of its molecular and electronic structure and constitutes one of the best experimental sources of information about the interaction of a solvated molecule with the surrounding molecular environment. An excellent example of the sensitivity of the nuclear shielding on the molecular environment is provided by the hydrogen selenide molecule, for which the shift in the selenium shielding is 7 ppm upon deuteration[1] and for which a gas-to-liquid shift of more than 100 ppm has been observed.[2,3] Selenium compounds are important in organic chemistry and biochemistry.[4–7] Owing to the rather high natural abundance of the spin-1/2 isotope ^{77}Se, it is readily observable with modern NMR techniques.[8,9] Furthermore, selenium has been successfully used as a surrogate probe for sulfur and oxygen in biological systems.[3]

The nuclear shielding of selenium in H_2Se has been investigated both experimentally[1,2,10–14] and theoretically.[3,15–21] The theoretical investigations have been concerned mainly with reproducing the ^{77}Se chemical shifts in the gas phase rather than with calculating the absolute shieldings or gas-to-liquid shifts. Basis-set and electron-correlation effects have therefore been the main consideration in these works. The reason for calculating gas-phase shifts is that the experimental absolute shielding scale for selenium has not been determined accurately. Absolute shielding scales are often determined by using experimental data for the paramagnetic contribution to the shielding, obtainable from spin-rotation constant measurements in microwave spectroscopy, and adding a theoretically determined diamagnetic part. However, the relativistic effect on the diamagnetic contribution to selenium is expected to be several hundred ppm,[22] making it difficult to arrive at a reliable theoretical estimate for this contribution.

During the last decade, there has been rapid progress in the *ab initio* calculation of nuclear shieldings (see Ref. 23), mainly due to efficient implementations of local gauge-origin methods using response theory[24–26] and the development of methods that include electron correlation.[25–28] Indirect spin–spin couplings can also be efficiently calculated within the framework of response theory.[29] Still, despite the recent progress in the development of theoretical methods for the calculation of these properties, the direct comparison with experiment remains difficult because of the large zero-point vibrational and temperature effects and because the molecular structure is perturbed by neighboring solvent molecules. Recently, solvent effects on nuclear shieldings have been calculated both by considering the surroundings as a continuous dielectric medium[30,31] and by studying clusters[30,32–34] (in the latter case, also by embedding the cluster in a dielectric medium[35]). However, both approaches represent rather crude approximations to the true interactions in the solvent and the results must be interpreted with care. The dielectric-medium

[a)]Permanent address: University of Oslo, Blindern, N-0315 Oslo, Norway.

model, for example, cannot take into account hydrogen bonding of the solute without explicitly adding the neighboring molecules. Likewise, there are difficulties associated with the cluster model as well. First, the basis-set superposition errors (BSSEs) may be large, as has been demonstrated for the shielding of the water dimer (see Ref. 36). Second, although the geometry of the cluster is important, a full optimization of the cluster geometry may be difficult because of the couplings between low-frequent (intermolecular) and high-frequent (intramolecular) motions. These problems are particularly troublesome since, because of the size of the clusters, only simple calculations (using small basis sets and noncorrelated models) may usually be carried out.

In this work, we investigate the gas-to-liquid shift of H_2Se using our recently developed MOSCF method for calculating nuclear shieldings and magnetizabilities using London atomic orbitals to ensure gauge-origin independent magnetic properties.[31] In addition, we present the theoretical framework needed for evaluating the solvent effects on a molecular property in the presence of triplet perturbation operators. In our model. the molecule is placed in a spherical cavity embedded in a homogeneous, isotropic, and linear dielectric medium. We compare our calculated shielding and spin–spin coupling constants of the solute with results obtained at the same level of theory for the gas-phase molecule.

The calculations presented here are not only the first *ab initio* calculations of the nuclear spin–spin couplings in H_2Se, but since the spin–spin couplings of H_2Se have been measured in only one solvent,[11–13] this work is the first attempt, both theoretically and experimentally, at investigating the solvent dependence of the spin–spin couplings in this molecule.

Broadly speaking, the response of a molecule to a dielectric medium is twofold: the electronic charge distribution is polarized and the geometry is altered. It should be noted, however, that a surrounding medium also affects the nuclear shielding in other ways and the total solvent effects are normally partitioned as[37]

$$\sigma_{\text{solvent}}=\sigma_b+\sigma_a+\sigma_E+\sigma_w, \tag{1}$$

where σ_b is proportional to the magnetic susceptibility, σ_a arises from the anisotropy of the magnetizabiltity of the neighboring molecules, σ_w is due to van der Waals interactions, and σ_E is due to electrostatic interactions. In the present investigation, we restrict ourselves to modeling σ_E with a dielectric medium. If we were to ascertain how close we are to experimentally observed solvent shifts, we would need to estimate the three other terms σ_b; σ_a, and σ_w in Eq. (1) as well. This would require a knowledge of the structure of the first solvation shell and dispersion interactions, which is beyond the scope of the present investigation. Also, we shall in this work assume that the relativistic effects on the selenium gas-to-liquid shift are small.

The bulk of this paper is organized as follows: We begin with a section describing the theoretical framework for calculating dielectric medium effects on a molecule perturbed by triplet operators. We then describe our investigations of basis-set and orbital-space requirements for an accurate description of the nuclear shieldings, the spin–spin coupling constants, and the structure of the H_2Se molecule. We then go on to consider the gas-phase properties of H_2Se comparing in particular our results with those of previous theoretical investigations. Finally, we discuss our results for H_2Se in the dielectric medium.

II. SPIN–SPIN COUPLINGS OF SOLVATED MOLECULES

The isotropic indirect spin–spin coupling J consists of four different contributions[38]

$$J=J_{\text{DSO}}+J_{\text{PSO}}+J_{\text{FC}}+J_{\text{SD}}, \tag{2}$$

where J_{DSO} is the diamagnetic and J_{PSO} the paramagnetic spin–orbit contributions, respectively. J_{FC} is the Fermi-contact, and J_{SD} the spin–dipole contributions. All these contributions have previously been implemented for MCSCF wave functions of molecules in the gas phase by Vahtras *et al.*[29]

The diamagnetic spin–orbit term is an expectation value of the operator

$$H_{\text{DSO}}=\frac{e^2\mu_0^2}{(4\pi)^2 2m_e}\sum_{n,N\neq M}\gamma_N\gamma_M \times\frac{(I_N\cdot I_M)(r_{nN}\cdot r_{nM})-(I_N\cdot r_{nM})(I_M\cdot r_{nN})}{r_{nM}^3 r_{nN}^3} \tag{3}$$

using the unperturbed electron density, and it can therefore be straightforwardly evaluated following Ref. 39 using the optimized electron density of the molecule in the dielectric medium. In Eq. (3) we have introduced the symbols e and m_e for the electronic charge and mass, respectively, μ_0 is the vacuum permeability, and γ_N and I_N are the magnetogyric ratio and nuclear spin of nucleus N.

The remaining three contributions to the spin–spin coupling constants can be calculated using linear response theory[40]

$$J^{\alpha}=\tfrac{1}{2}\langle\langle H^{\alpha};H^{\alpha}\rangle\rangle_{\omega=0}, \tag{4}$$

where the perturbing operators H^{α} are either PSO, SD, or FC. $\langle\langle\ ;\ \rangle\rangle$ is in this equation the linear response function. The perturbing operators in Eq. (4) are given as

$$H_{\text{PSO}}=\frac{e\mu_0}{4\pi m_e}\sum_{n,N}\gamma_N I_N\frac{l_{nN}}{r_{nN}^3}, \tag{5}$$

$$H_{\text{SD}}=\frac{\mu_B g_e\mu_0}{h4\pi}\sum_{n,N}\gamma_N\frac{3(s_n\cdot r_{nN})(r_{nN}\cdot I_N)-r_{nM}^2 s_n\cdot I_N}{r_{nN}^5}, \tag{6}$$

and

$$H_{\text{FC}}=\frac{2\mu_B g_e\mu_0}{3h}\sum_{n,N}\gamma_N\delta(r_{nN})s_n\cdot I_N, \tag{7}$$

where the Bohr magneton is denoted by μ_B. The electronic spin of electron n is given by s_a and the orbital angular momentum of electron n with respect to nuclens N is given by

$$l_{nN}=r_{nN}\times p_n, \tag{8}$$

where p_n is the momentum of electron n.

In the solvent model we use in this work, the solvated molecule is contained in a spherical cavity, embedded in a dielectric medium. The charge distribution of the solute induces polarization moments in the dielectric medium, the induced polarization moments being described by the polarization vector relation

$$\mathbf{P}^{\mathrm{tot}}=\mathbf{P}^{\mathrm{in}}+\mathbf{P}^{\mathrm{op}}, \tag{9}$$

where $\mathbf{P}^{\mathrm{tot}}$ is the total polarization vector; $\mathbf{P}^{\mathrm{in}}$ is the inertial polarization vector related to the static dielectric constant (ϵ_{st}); and $\mathbf{P}^{\mathrm{op}}$ is the optical polarization vector which is related to the optical dielectric constants (ϵ_{op}).

On the time scale relevant for NMR experiments, we may consider all degrees of freedom of the solvent to be able to relax and equilibrate with respect to the charge distribution of the solute. Therefore we only use the static dielectric constant to describe the polarization of the surrounding medium. This leads to the following energy expression for the solvated system in the presence of the external magnetic field[31]

$$E_{\mathrm{tot}}=E_{\mathrm{vac}}+E_{\mathrm{sol}}, \tag{10}$$

where E_{vac} is the vacuum energy and E_{sol} is the dielectric polarization energy given by

$$E_{\mathrm{sol}}=\sum_{lm} R_{lm}(\rho,\epsilon_{\mathrm{st}})\langle T_{lm}(\rho)\rangle. \tag{11}$$

The response of the dielectric medium can in the case of a spherical cavity be written

$$R_{lm}(\rho,\epsilon_{\mathrm{st}})=g_l(\epsilon_{\mathrm{st}})\langle T_{lm}(\rho)\rangle, \tag{12}$$

where the factor $g_l(\epsilon_{\mathrm{st}})$ is

$$g_l(\epsilon_{\mathrm{st}})=\frac{1}{2}\,a^{-(2l+1)}\,\frac{(l+1)(\epsilon_{\mathrm{st}}-1)}{l+\epsilon_{\mathrm{st}}(l+1)}. \tag{13}$$

In deriving these equations we have performed a multipole expansion of the solutes charge distribution, denoting the charge moments by $\langle T_{lm}(\rho)\rangle$. These charge moments are expressed as expectation values of the nuclear (T^n_{lm}) and electronic (T^e_{lm}) solvent operators

$$\langle T_{lm}\rangle=T^n_{lm}-\langle T^e_{lm}\rangle, \tag{14}$$

$$T^e_{lm}=t^{lm}(r)=\sum_{rs} t^{lm}_{rs}E_{rs}, \tag{15}$$

$$T^n_{lm}=\sum_b Z_b t^{lm}(R_b), \tag{16}$$

where Z_b (R_b) is the nuclear charge (position vector) of nucleus b. The subscripts r and s represent the orbitals ϕ_r and ϕ_s and the excitation operator E_{rs} is

$$E_{rs}=\sum_\sigma a^\dagger_{r\sigma}a_{s\sigma}, \tag{17}$$

where we sum over the spin quantum number σ. The creation and annihilation operators for an electron in spin–orbital $\phi_{r\sigma}$ are denoted $a^\dagger_{r\sigma}$ and $a_{r\sigma}$. The functions $t^{lm}(Rg)$ and t^{lm}_{rs} are defined through the conventional spherical harmonics, S^μ_l, where μ is a positive integer[41,42]

$$\begin{aligned} l^{l0}&=S^0_l,\\ l^{l\mu}&=\sqrt{1/2}(S^\mu_l+S^{-\mu}_l)\\ l^{l-\mu}&=-i\sqrt{1/2}(S^\mu_l-S^{-\mu}_l). \end{aligned} \tag{18}$$

Following Ref. 42, we assume that our system is described by a multiconfiguration self-consistent reaction-field (MCSCRF) wave function and that it satisfies the generalized Brillouin theorem

$$\begin{pmatrix} \langle O|[q^\dagger_{rs}, & H_0+W_{\mathrm{sol}}]|O\rangle \\ \langle O|[R^\dagger_n, & H_0+W_{\mathrm{sol}}]|O\rangle \end{pmatrix}=\begin{pmatrix}0\\0\end{pmatrix}, \tag{19}$$

where the Hamiltonian H_0 is the usual Hamiltonian for a many-electron system in vacuum. W_{sol} is the solvent contribution which can be written as[43,44]

$$\begin{aligned} W_{\mathrm{sol}}=&2\sum_{lm,rs,r's'} g_l(\epsilon_{\mathrm{st}})t^{lm}_{rs}E_{rs}|O\rangle\langle O|t^{lm}_{r's'}E_{r's'}\\ &-2\sum_{lm,rs} g_l(\epsilon_{\mathrm{st}})T^n_{lm}t^{lm}_{rs}E_{rs}+\sum_{lm} g_l(\epsilon_{\mathrm{st}})T^m_{lm}T^n_{lm}. \end{aligned} \tag{20}$$

We let the MCSCRF state be parametrized as

$$|O\rangle=\sum_g C_g|\Phi_g\rangle, \tag{21}$$

where $|\Phi_g\rangle$ is a set of configuration state functions (CSFs) and where the CSF is a linear combination of Slater determinants

$$|\Phi_g\rangle=\prod_r a^\dagger_r|\mathrm{vac}\rangle. \tag{22}$$

We have in the above equations also introduced

$$q^\dagger_{rs}=a^\dagger_r a_s, \quad r>s \tag{23}$$

and

$$R^\dagger_n=|n\rangle\langle O|, \tag{24}$$

where $|n\rangle$ denotes the orthogonal complement space to $|O\rangle$ spanned by $|\Phi_g\rangle$. The evolution of the reference state is determined by requiring that Ehrenfest's theorem be satisfied through each order in the interaction operator:

$$\frac{d}{dt}\langle T^t\rangle=\left\langle\frac{dT^t}{dL}\right\rangle-i\langle[T^t,H]\rangle, \tag{25}$$

where

$$H=H_0+W_{\mathrm{sol}}+V_{\mathrm{pert}}(t), \tag{26}$$

where $V_{\mathrm{pert}}(l)$ is the external perturbation and T^t is given in Eq. (30). The molecular system relaxes as a result of the external perturbation and the state may be parametrized as[40]

$$|O^t\rangle=e^{ik(t)}e^{iS(t)}|O\rangle, \tag{27}$$

where $e^{ik(t)}$ describes a unitary transformation in orbital space

$$k=\sum_{rs}\ (\kappa_{rs}(t)a_r^\dagger a_s+\kappa'_{rs}(t)a_s^\dagger)$$

$$=\sum_{k}\ (\kappa_k(t)q_k^\dagger+\kappa'_k(t)q_k) \tag{28}$$

and $e^{iS(t)}$ a unitary transformation in configuration space

$$S(t)=\sum_{n}\ (S_n(t)R_n^+ +S'_n(t)R_n). \tag{29}$$

The parameters $\kappa_k(t)$, $\kappa'_k(t)$, $S_n(t)$, and $S'_n(t)$ determine the time evolution of the wave function. We use the following set of operators to describe how the solvated system evolves

$$T=q_i^\dagger,R_i^\dagger,q_i,R_i \tag{30}$$

and these operators are collected in a row vector. The orbital operators are given as

$$q_i^\dagger=a_{r\alpha}^\dagger a_{s\alpha}\pm a_{r\beta}^\dagger a_{s\beta} \tag{31}$$

and

$$q_i=a_{s\alpha}a_{r\alpha}\pm a_{s\beta}^\dagger a_{r\beta}, \tag{32}$$

where the top symbol or sign refers to the singlet case and the bottom to the triplet case. A general vector in this basis is written as a column vector

$$N=\begin{pmatrix} k_j \\ S_j \\ k'_j \\ S'_j \end{pmatrix}. \tag{33}$$

Thus N, may refer to an orbital rolation parameter or a configuration parameter.

As shown in Ref. 45, the triplet linear response function for a MCSCRF state has the same structure as the vacuum linear response function, the only change being that additional terms are added to the Hessian-type matrix $E^{[2]}$. When solving linear response eigenvalue or linear equations using iterative techniques, linear transformations with the Hessian-type matrix on trial vectors $E^{[2]}N$ are required. The linear transformed vectors then contain in addition to the vacuum contributions also contributions originating from the solvent. These contributions are for the q_j components given by

$$E^{[2]}(q_j)=-\langle O^L|[^-q_j,T_g]|O\rangle+\langle O|[^-q_j,T_g]|O^R\rangle$$
$$-\langle O|[^-q_j,T_{y0}]|O\rangle-\langle O|[^-q_j,T_{x0}]|O\rangle$$
$$-\langle O|[^-q_j,T_{xc}]|O\rangle, \tag{34}$$

for $q_j^\dagger$ by

$$E^{[2]}(q_j^+)=-\langle O^L|[^-q_j^\dagger,T_g]|O\rangle+\langle O|[^-q_j^\dagger,T_g]|O^R\rangle$$
$$-\langle O|[^-q_j^\dagger,T_{y0}]|O\rangle-\langle O|[^-q_j^\dagger,T_{x0}]|O\rangle$$
$$-\langle O|[^-q_j^\dagger,T_{xc}]|O\rangle, \tag{35}$$

for R_j by

$$E^{[2]}(R_j)=-\langle j|T_g|O^R\rangle+\langle O|T_g|O\rangle S_j-\langle j|^-T_{y0}|O\rangle$$
$$-\langle j|^-T_{x0}|O\rangle-\langle j|^-T_{xc}|O\rangle, \tag{36}$$

and finally $R_j^\dagger$ is described by

$$E^{[2]}(R_j^\dagger)=-\langle O^L|T_g|j\rangle-\langle O|T_g|O\rangle S'_j+\langle O|^-T_{y0}|j\rangle$$
$$+\langle O|^-T_{x0}|j\rangle-\langle O|^-T_{xc}|j\rangle, \tag{37}$$

where we have indicated the triplet operators with the superscript minus. The effective operators are defined as

$$T_g=-2\sum_{lm,rs}\ g_l(\epsilon)\langle T_{lm}\rangle t_{rs}^{lm}E_{rs}, \tag{38}$$

$$T_{y0}=-2\sum_{lm,rs}\ g_l(\epsilon)\langle T_{lm}\rangle Q_{rs}^{lm}E_{rs}, \tag{39}$$

$$T_{x0}=2\sum_{lm,rs}\ g_l(\epsilon)\langle Q_{lm}\rangle t_{rs}^{lm}E_{rs}, \tag{40}$$

$$T_{xc}=2\sum_{lm,rs,r's'}\ g_l(\epsilon)t_{r's'}^{lm}t_{rs}^{lm}(\langle {}^LO|E_{rs}|O\rangle$$
$$+\langle O|E_{rs}|O^R\rangle)E_{r's'}, \tag{41}$$

where

$$|O^R\rangle=-S_nR_n^+|O\rangle=-S_n|n\rangle \tag{42}$$

and

$$\langle {}^LO|=\langle O|(S'_nR_n^+)=S'_n\langle n|. \tag{43}$$

The one-index transformed solvent integrals are given as

$$\sum_{rs}\ [k(t),t_{rs}^{lm}E_{rs}]=\sum_{rs}\ Q_{rs}^{lm}E_{rs}, \tag{44}$$

where

$$Q_{rs}^{lm}=\sum_{t}\ [k_{rt}t_{ts}^{lm}-t_{rt}^{lm}k_{ts}]. \tag{45}$$

For further details we refer to Refs. 29, 40, 43, and 45. With the presented formalism we have developed a method for obtaining molecular properties involving triplet electronic properties. Previously, the solvent response methodology has only been presented for molecular properties involving singlet electronic properties and triplet excitation energies.

III. COMPUTATIONAL DETAILS

In this work, we employ the atomic natural orbital (ANO) basis sets by Pierloot *et al.*,[46] which for molecular magnetic properties have shown to give excellent results.[47–50] We denote the contractions of the primitive ANO basis by, for example, ANO[$5s4p3d/2s1p$], where $5s4p3d$ is the contraction of the ($17s15p9d$) primitive selenium set and $2s1p$ the contraction of the ($7s3p$) primitive hydrogen set. The primitive (decontracted) set is referred to simply as ANO. The various extensions to the primitive ANO set are denoted by, for instance, ANO+Se: $1f$, indicating that the selenium basis has been extended with one f function. In the restricted active space SCF (RASSCF) approach,[51,52] the molecular orbitals are partitioned into five different spaces:

(1) The inactive space. This space contains all orbitals that are doubly occupied in all configurations. In this space, we include the $1s-3d$ orbitals on selenium.

TABLE I. Basis-set dependence of the nuclear shieldings and spin–spin couplings of H_2Se at the SCF level.

	σ^{Sc}/ppm	σ^{H}/ppm	$^1J^{SeH}$/Hz	$^2J^{HH}$/Hz
ANO[5*s*4*p*3*d*/2*s*1*p*]	2259.2	30.28	159.6	−29.6
ANO[6*s*5*p*4*d*/3*s*2*p*]	2226.2	30.65	122.8	−25.1
ANO[7*s*6*p*5*d*/4*s*3*p*]	2226.4	30.55	167.9	−21.0
ANO	2167.8	30.53	103.0	−21.6
ANO+Se:1*s*[a]	2167.8	30.53	103.0	−21.6
ANO+Se:1*p*[a]	2167.8	30.53	103.0	−21.6
ANO+Se:1*d*[a]	2166.6	30.53	102.9	−21.6
ANO+Se:1*f*[b]	2170.4	30.46	100.1	−22.0
ANO+Se:2*f*[c]	2165.6	30.37	100.4	−22.2
ANO+H:1*s*[a]	2167.8	30.53	103.0	−21.6
ANO+H:1p[a]	2167.8	30.53	103.0	−21.6

[a]Extra diffuse functions have been added according to a geometric series.
[b]The exponent is 0.25.
[c]The exponents are 0.35 and 1.40.

(2) The RAS1 space. From this space, only a restricted number of electrons are allowed to be excited in any configuration. In this work, we do not use the RAS1 space.

(3) The RAS2/active space. A full Cl optimization is carried out in the space spanned by the orbitals of the RAS2/active space.

(4) The RAS3 space. This space consists of orbitals into which a restricted number of electrons is allowed to be excited. In all our calculations, the maximum number of electrons allowed to be excited into the RAS3 space is two.

(5) The virtual space. This space contains the orbitals that are unoccupied in all configurations.

In the following, we denote our wave functions by $^{\text{inactive}}\text{CAS}^{\text{active}}$ and $^{\text{inactive}}_{\text{RAS1}}\text{RAS}^{\text{RAS2}}_{\text{RAS3}}$, where the superscripts and subscripts give the numbers of orbitals in each space. For each space, four numbers are given, corresponding to the number of orbitals in each irreducible representation.

The experimental gas-phase geometry has been taken from Ref. 53, where $r_{\text{SeH}}=1.460$ Å and $\angle_{\text{HSeH}}=90.9°$. For the geometry optimization of the gas-phase molecule and for the molecule in the dielectric medium, we have used the second-order methods described in Refs. 54 and 55. In the study of the solvated molecule, we have optimized the geometries and calculated the shielding and spin–spin coupling constants for the following dielectric constants: $\varepsilon=2.209$ (1,4-dioxane), $\varepsilon=6.02$ (ethyl acetate), $\varepsilon=13.3$ (l-hexanol), $\varepsilon=32.63$ (methanol), and $\varepsilon=78.54$ (water). In all these calculations, the cavity radins has been kept fixed at 4.9 bohrs, corresponding to the distance from the center of mass of the molocule to the hydrogen plus the van-der-Waals radius of the hydrogen atom (1.1 Å).

TABLE III. Basis-set dependence of the Fermi-contact term to the spin–spin couplings at the SCF level.[a]

	$^1J^{SeH}_{FC}$/Hz	$^2J^{HH}_{FC}$/Hz
ANO	88.8	−21.5
ANO+Se:1*S*	90.1	−21.5
ANO+Se:2*S*	90.7	−21.5
ANO+Se:3*S*	90.8	−21.5
ANO+H:1*S*	92.5	−23.4
ANO+H:2*S*	94.0	−24.1
ANO+H:3*S*	94.6	−24.4

[a]*s* functions with large exponents have been added according to a geometric series.

IV. BASIS SET AND CORRELATION EFFECTS

The Hartree–Fock (HF) results are presented in Table I for the nuclear shieldings and for the total spin–spin couplings, and in Table II for the individual contributions to the spin–spin coupling constants. The basis-set convergence of the Fermi-contact (FC) term has been investigated in more detail by adding *s* functions with larger exponents to improve the description of the charge distribution at the nuclei, see Table III.

For the selenium shielding, we note a difference between the contracted and primitive ANO basis sets of more than 60 ppm (see Table I). The addition of diffuse functions give a change in the shielding of only a few ppm, the largest change coming from the diffuse *f* functions. In contrast, the proton shielding varies only with a few tenths of a ppm among the basis sets investigated. As for the selenium shielding, the most important shift in the hydrogen shielding comes from the addition of diffuse *f* functions to the selenium basis.

For the selenium-proton spin–spin coupling $^1J^{SeH}$, large contraction errors are found for the contracted basis sets. This is to be expected since contraction reduces the flexibility of the core orbitals as observed in a recent systematic investigation of basis-set requirements for calculations of spin–spin coupling constants.[56] The additional *f* functions give substantial contributions to the FC terms (see Table II), the remaining diffuse functions producing negligible effects. From Table III, we also note that, for the FC terms, the *s* functions added to the primitive set lead to large changes.

TABLE II. Basis set dependence of the different contributions to the spin–spin couplings at the SCF level.

	$^1J^{SeH}_{DSO}$/Hz	$^1J^{SeH}_{PSO}$/Hz	$^1J^{SeH}_{SD}$/Hz	$^1J^{SeH}_{FC}$/Hz	$^2J^{HH}_{DSO}$/Hz	$^2J^{HH}_{PSO}$/Hz	$^2J^{HH}_{SD}$/Hz	$^2J^{HH}_{FC}$/Hz
ANO[5*s*4*p*3*d*/2*s*1*p*]	0.0	10.0	−2.0	151.6	−1.7	1.4	0.1	−29.3
ANO[6*s*5*p*4*d*/3*s*2*p*]	0.0	15.7	−3.6	110.7	−1.7	1.3	0.2	−24.9
ANO[7*s*6*p*5*d*/4*s*3*p*]	0.0	15.5	−3.0	155.4	−1.7	1.3	0.2	−20.8
ANO	0.0	17.1	−2.9	88.8	−1.7	1.4	0.2	−21.5
ANO+Se:1*f*[a]	0.0	17.2	−3.1	86.0	−1.7	1.6	0.1	−22.0
ANO+Se:2*f*[b]	0.0	16.8	−3.0	86.6	−1.7	1.7	0.1	−22.2

[a]The exponent is 0.25.
[b]The exponents are 0.35 and 1.40.

TABLE IV. Basis-set dependence of the dipole moment and the harmonic frequencies at the SCF level.

	μ/D	ω_1/cm^{-1}	ω_2/cm^{-1}	ω_3/cm^{-1}
ANO[$5s4p3d/2s1p$]	0.831	2590.07	1175.13	2596.26
ANO[$6s5p4d/3s2p$]	0.783	2549.91	1170.09	2556.18
ANO[$7s6p5d/4s3p$]	0.787	2546.93	1167.36	2553.07
ANO	0.789	2544.60	1168.09	2550.45
ANO+Se:$1s$	0.789	2544.64	1168.09	2550.51
ANO+Se:$1f$[a]	0.807	2541.67	1167.43	2547.05
ANO+Se:2[b]	0.786	2538.61	1167.45	2543.24

[a]The exponent is 0.25
[b]The exponents are 0.35 and 1.40.

TABLE V. Electron correlation dependence of shieldings and spin–spin couplings. The ANO[$6s5p4d/3s2p$] basis set has been used.

	σ^{Se}/ppm	σ^{H}/ppm	$^1J^{SeH}$/Hz	$^2J^{HH}$/Hz
HF	2226.2	30.65	122.8	−25.1
^{7331}CAS^{1221}	2319.1	30.79	138.7	−20.1
^{7331}CAS^{6331}	2320.7	30.62	130.2	−18.8
^{7331}RAS$^{4221}_{2110}$	2321.1	30.63	129.5	−18.8
^{7331}RAS$^{4221}_{4221}$	2295.2	30.94	128.2	−16.7
^{7331}RAS$^{4221}_{7532}$	2279.7	31.09	131.8	−16.4
^{7331}RAS$^{4221}_{11;753}$	2282.0	31.10	n.c.[a]	n.c[a]

[a]Not calculated.

The dipole moment and harmonic frequencies display reasonable results for all basis sets except for the smallest contraction (Table IV). To assess the importance of electron correlation, we have investigated the convergence of the properties with respect to various extensions of the MCSCF orbital spaces using the ANO[$6s5p4d/3s2p$] basis set, see Table V. The selenium shielding has converged to within a few ppm for the largest RAS spaces and the proton shielding to within 0.01 ppm. The spin–spin couplings display a pronounced correlation dependence but, as seen in Table VI, we need only consider the FC term beyond the smallest RAS spaces.

The electron-correlation dependence of the FC terms has been further investigated with a larger ANO basis set, see Table VII. The uncontracted selenium basis was extended with an f function and a tight s function, and the hydrogen basis with one diffuse s function and two core s functions. This basis will be denoted ANO-fc. We note that the convergence is somewhat slow. As shown in Table VIII, correlation effects on the dipole moment and harmonic frequencies are also substantial.

Because of the difference in cost of the various properties, and in particular the cost of the different contributions to the spin–spin coupling constants with regard to their overall importance, we have, based on our basis-set and orbital-space investigations, adopted the following wave functions for the remaining calculations: For the geometry optimziations we use the ^{7331}RAS$^{4221}_{4221}$ orbitals space together with the ANO[$6s5p4d/3s2p$] basis set. In the calculations of the nuclear shieldings, we use the ^{7331}RAS$^{4221}_{7532}$ orbital space together with the primitive ANO basis set. For all contributions to the spin–spin coupling constants other than the Fermi-contact term, we use the ^{7331}RAS$^{4221}_{4221}$ orbital space together with the primitive ANO basis. For the Fermi-contact contribution to the spin–spin coupling constants we have used the ^{7331}RAS$^{4221}_{7532}$ orbital space and the ANO-fc basis set.

V. GAS-PHASE PROPERTIES

The optimized gas-phase geometry is in excellent agreement with the experimental geometry,[53] the optimized bond distance being 1.474 Å and the bond angle 90.0°. Somewhat surprisingly, therefore, the difference between the selenium shielding calculated using the experimental and the optimized gas-phase geometrics is substantial. As seen from Table IX, the calculated value for the experimental geometry is 2280 ppm as opposed to 2198 ppm at the optimized geometry, a difference of 82 ppm. Considering the individual tensor components of the selenium shielding (defined relative to the isotropic shielding) in Table IX, the geometry shifts are smaller, but still substantial. The largest effect is noted for the component along the dipole axis (aa), which changes by about 30 ppm. Consequently, also the anisotropy of the selenium shielding is sensitive to the molecular geometry.

In Table IX, our results for the selenium shielding are compared with other theoretical results. Our best result is 15 ppm lower than the singles and doubles coupled-cluster (CCSD) result of Bühl, Gauss, and Stanton,[19] which we consider to be the most accurate of the previous calculations. The differences with the other calculations are substantially larger. We note, however, that a direct comparison is made difficult by the use of different geometries in the different calculations. In view of the strong geometry dependence observed for the shielding, these geometrical effects may be as important as the correlation effects for the shielding. The agreement with the experimentally determined shielding components[2] is far from satisfactory. However, since the ex-

TABLE VI. Electron correlation dependence of the different contributions to the spin–spin couplings. The ANO[$6s5p4d/3s2p$] basis set has been used.

	$^1J^{SeH}_{DSO}$/Hz	$^1J^{SeH}_{PSO}$/Hz	$^1J^{SeH}_{SD}$/Hz	$^1J^{SeH}_{FC}$/Hz	$^2J^{HH}_{DSO}$/Hz	$^2J^{HH}_{PSO}$/Hz	$^2J^{HH}_{SD}$/Hz	$^2J^{HH}_{FC}$/Hz
HF	0.0	15.7	−3.6	110.7	−1.7	1.3	0.2	−24.9
^{7331}CAS^{4221}	0.0	16.8	−1.8	123.7	−1.7	1.3	0.1	−19.9
^{7331}CAS^{6331}	0.0	16.3	−1.5	115.4	−1.7	1.3	0.1	−18.6
^{7331}RAS$^{4221}_{2110}$	0.0	16.3	−1.5	114.8	−1.7	1.4	0.1	−18.6
^{7331}RAS$^{4221}_{4221}$	0.0	16.6	−1.4	113.0	−1.7	1.3	0.1	−16.5
^{7331}RAS$^{4221}_{7532}$	0.0	16.7	−1.3	116.4	−1.7	1.3	0.1	−16.2

TABLE VII. Electron correlation dependence of the Fermi-contact term. The ANO-fc basis set has been employed.

	$^1J_{FC}^{SeH}$/Hz	$^2J_{FC}^{HH}$/Hz
HF	92.2	−24.6
$^{7331}CAS^{4221}$	103.2	−19.5
$^{7331}RAS^{4221}_{2110}$	91.2	−18.2
$^{7331}RAS^{4221}_{4221}$	96.7	−16.2
$^{7331}RAS^{4221}_{7532}$	98.0	−15.6
$^{7331}RAS^{4221}_{11;753}$	99.8	−15.2

periment has been carried out in the solid state, the difference in geometries in the gas and solid phases may account for most of this discrepancy.

The optimized geometry gives a proton shielding 0.5 ppm lower than the shielding calculated for the experimental gas-phase geometry. This is a relatively large shift for a proton, indicating that, for this system, the proton shift is sensitive to the molecular geometry. As demonstrated in several investigations,[57–59] the indirect spin–spin couplings are very sensitive to changes in the molecular geometry. This is true also for the spin–spin couplings in hydrogen selenide, where, for the $^1J^{SeH}$ coupling, we obtain 113.6 Hz at the experimental geometry and 106.3 Hz at the optimized geometry. Not surprisingly, the largest contribution to the geometry dependence comes from the FC term, which changes by 9 Hz upon geometry optimization. The PSO and SD terms also change quite substantially upon optimization, each by about 1 Hz.

For the $^2J^{HH}$ indirect spin–spin coupling, the gas-phase geometry gives a coupling constant of −15.8 Hz and the optimized geometry a coupling of −16.5 Hz. As for $^1J^{SeH}$, the FC term gives the largest contribution to this shift (1 Hz), although, for this coupling, the DSO term also shows a quite substantial shift (of about 0.3 Hz). In contrast, the PSO and SD terms hardly change upon optimization of the geometry.

VI. SOLVENT EFFECTS

The optimized structures obtained for the different dielectric constants are collected in Table X. The bond distance becomes slightly shorter when the molecule is put in a dielectric medium but increases with increasing dielectric constant. All the effects are, however, within 0.002 Å. The bond angle increases by 1.8° when the molecule is placed in a dielectric medium and increases by an additional 0.3° for the dielectric constant of water. The major effect of the dielectric medium on the structure of H_2Se is thus to increase the bond angle.

In the Onsager model (dipole approximation), it is expected that the bond distance increases and the bond angle decreases when H_2Se is solvated, in order for the molecule to increase its dipole moment. It is therefore interesting to note that, for H_2Se, the higher-order charge moments dominate and counteract the effects of the dipole moment as observed previously.[31]

In Fig. 1, where we have plotted the changes in the nuclear shielding of selenium relative to the gas-phase value for the various dielectric constants, we see that the solvent shift of the selenium shielding is about 40 ppm and in the same direction as observed in experiment.[2,3] However, a direct comparison with experiment is difficult since the temperature and pressure dependences are strong for the selenium shift.[2] In the case of H_2Se, liquid H_2Se is shifted with 127 ppm in comparison to gaseous H_2Se at 5 atm and 293 K.[2] The tensor components (relative to the isotropie shielding) also change substantially when the molecule is embedded in a dielectric medium. The component along the dipole axis (aa) increases by about 60 ppm, whereas the other in-plane component (bb) decreases by about 10 ppm and the out-of-plane component decreases by about 50 ppm. The *aa* component of the shielding thus shows good agreement with experiment [−259 ppm compared with the experimental value of −240.7 ppm (Ref. 2)], whereas the other two com-

TABLE IX. Gas-phase selenium shieldings. The components are given relative to the isotropic value. σ_{aa} corresponds to the value along the dipole axis, σ_{bb} to the value in the molecular plane, and σ_{cc} to the value perpendicular to the plane.

Method	σ^{Se}/ppm	σ^{Se}_{aa}/ppm	σ^{Se}_{bb}/ppm	σ^{Se}_{cc}/ppm
$^{7331}RAS^{4221}_{7532}$/ANO[a]	2280	−291	371	−83
$^{7331}RAS^{4221}_{7532}$/ANO[b]	2198	−320	398	−77
CCSD/[10*s*9*p*5*d*2*f*/3*s*1*p*][c]	2213	−286	401	−125
MP2/[10*s*9*p*5*d*2*f*/3*s*1*p*][d]	2236	−255	383	−128
SCF/[10*s*9*p*5*d*2*f*/3*s*1*p*][d]	2166	−344	444	−100
MP2/[8*s*6*p*3*d*1*f*/3*s*1*p*][e]	2276	−233	378	−145
DFT/uncontracted STO[f]	2093	−303	428	−125
Experimental (solid state)[g]		−240.7	250.2	−9.5

[a]Gas-phase geometry.
[b]Optimized geometry.
[c]See Ref. 19.
[d]See Ref. 20.
[e]See Ref. 17.
[f]See Ref. 21.
[g]See Ref. 2.

TABLE VIII. Electron correlation dependence of the dipole moment and harmonic frequencies. The ANO[6*s*5*p*4*d*/3*s*2*p*] basis set has been used.

	μ/D	ω_1/cm^{-1}	ω_2/cm^{-1}	ω_3/cm^{-1}
HF	0.783	2549.91	1170.09	2556.18
$^{7331}CAS^{4221}$	0.724	2452.67	1028.68	2498.83
$^{7331}CAS^{6331}$	0.816	2499.69	1040.96	2508.44
$^{7331}RAS^{4221}_{2110}$	0.811	2499.67	1041.21	2508.34
$^{7331}RAS^{4221}_{4221}$	0.693	2484.60	1044.38	2499.77
$^{7331}RAS^{4221}_{7532}$	0.637	2489.94	1055.95	2502.00

TABLE X. Dielectric effects on the geometry and dipole moment.

ϵ	r_{SeH}/Å	$\angle_{H\,SeH}$	μ/D
1	1.4736	89.95°	0.673
2.209	1.4717	91.75°	0.791
6.02	1.4727	91.93°	0.908
13.3	1.4733	92.01°	0.960
32.63	1.4735	92.05°	0.989
78.54	1.4737	92.07°	1.001

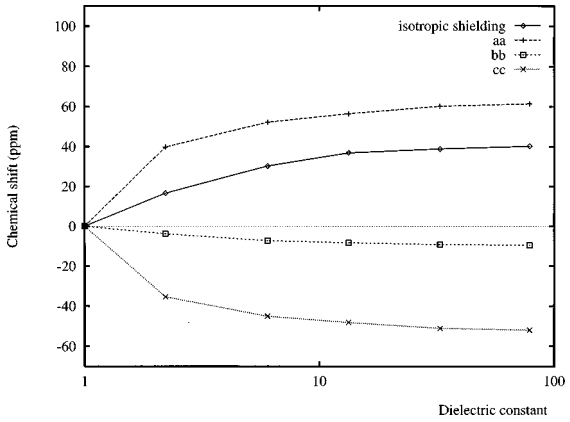

FIG. 1. Selenium shielding as a function of the dielectric constant. $\sigma^{\mathrm{Se}}(\epsilon=1)=2197.5$ ppm, $\sigma^{\mathrm{Se}}_{aa}(\epsilon=1)=-320.5$ ppm, $\sigma^{\mathrm{Se}}_{bb}(\epsilon=1)=397.8$ ppm, and $\sigma^{\mathrm{Se}}_{cc}(\epsilon=1)=-77.2$ ppm.

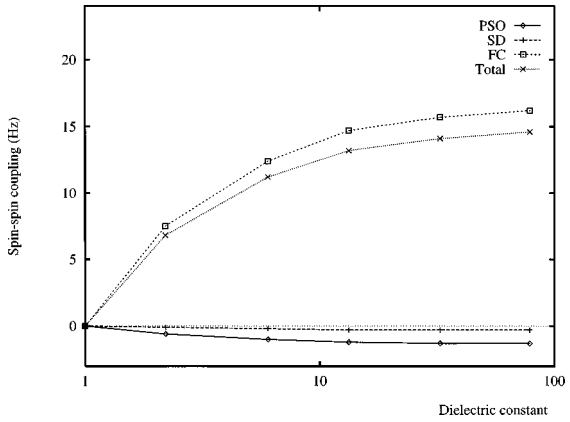

FIG. 3. Selenium-proton spin–spin coupling as a function of the dielectric constant. The DSO term is negligible for all dielectric constants. ${}^1J^{\mathrm{SeH}}_{\mathrm{PSO}}(\epsilon=1)=17.8$ Hz, ${}^1J^{\mathrm{SeH}}_{\mathrm{SD}}(\epsilon=1)=-0.7$ Hz, ${}^1J^{\mathrm{SeH}}_{\mathrm{FC}}(\epsilon=1)=89.2$ Hz, and ${}^1J^{\mathrm{SeH}}(\epsilon=1)=106.3$ Hz.

ponents shift away from the experiment when a dielectric medium is added, the difference from experiment being more than 100 ppm.

It is important to realize that the experimental tensor components are obtained in solid-state investigations. The solid state gives rise to directional crystal fields, which are very different from the polarization fields arising from the induced charge moments in the dielectric medium. Therefore we do not expect to obtain the same solvent shifts as those reported from the solid-state investigations; a better agreement should be obtained using methods designed to model the solid state[60] and intermolecular interactions.[36,61]

The solvent effect on the proton shielding is about -0.5 ppm, see Fig. 2. The tensor components (relative to the isotropic shielding) are presented as the out-of-plane component $\sigma^{\mathrm{H}}_{\mathrm{op}}$, one component almost parallel to the SeH bond $\sigma^{\mathrm{H}}_{\parallel}$, and one component almost perpendicular to the SeH bond, $\sigma^{\mathrm{H}}_{\perp}$. In Fig. 2, it is observed that $\sigma^{\mathrm{H}}_{\mathrm{op}}$ is almost constant, whereas $\sigma^{\mathrm{H}}_{\parallel}$ increases by about 0.5 ppm and $\sigma^{\mathrm{H}}_{\perp}$ by about the same amount. Since we present values relative to the isotropic shielding and since σ^{H} decreases by about 0.5 ppm, we conclude that $\sigma^{\mathrm{H}}_{\parallel}$ is virtually unchanged, that $\sigma^{\mathrm{H}}_{\mathrm{op}}$ decreases by $\sim$0.5 ppm and $\sigma^{\mathrm{H}}_{\perp}$ by $\sim$1 ppm.

For the indirect spin–spin coupling constants. the dominating solvent shift arises from changes in the FC term, see the ${}^1J^{\mathrm{SeH}}$ coupling in Fig. 3. The changes in the DSO term are negligible and not included in this figure. The changes in the SD term are also small, whereas the PSO term gives a significant contribution to the solvent shift of the order of a few Hz. For each of the dielectric constants, we have also calculated the FC term at the optimized gas-phase geometry. In Fig. 4, these results are compared with those obtained with the geometry optimized in the dielectric medium. The geometry effects are small, that is, the solvent effect on ${}^1J^{\mathrm{SeH}}$ arises mainly from the polarization of the charge distribution. ${}^1J^{\mathrm{SeH}}$ has been measured in the liquid phase to 63.4 ± 0.5 Hz[11] and for SeHD in 30% CH_2Cl_2 at $-56°$ C to 65.4 ± 0.2 Hz.[12] We obtain a gas-phase value of 106.3 Hz and a solvent shift of about 15 Hz but in the wrong direction relative to experiment. However, relativistic effects are likely to reduce this constant,[62] possibly improving the agreement with experiment.

The solvent effect on ${}^2J^{\mathrm{HH}}$ is illustrated in Fig. 5. The total contribution is about 1 Hz compared to the gas-phase value of -16.5 Hz. The PSO and DSO terms both give significant contributions, whereas the SD term is negligible. As

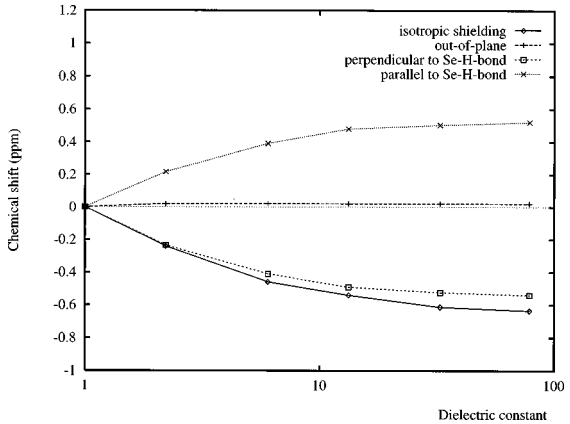

FIG. 2. Proton shielding as a function of the dielectric constant. $\sigma^{\mathrm{H}}(\epsilon=1)=30.629$ ppm, $\sigma^{\mathrm{H}}_{\mathrm{op}}(\epsilon=1)=-8.581$ ppm, $\sigma^{\mathrm{H}}_{\perp}(\epsilon=1)=-5.174$ ppm, and $\sigma^{\mathrm{H}}_{\parallel}(\epsilon=1)=13.755$ ppm.

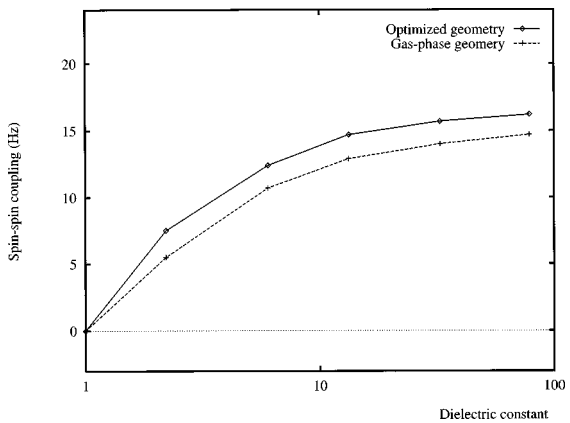

FIG. 4. Selenium-proton Fermi-contact term as a function of the dielectric constant.

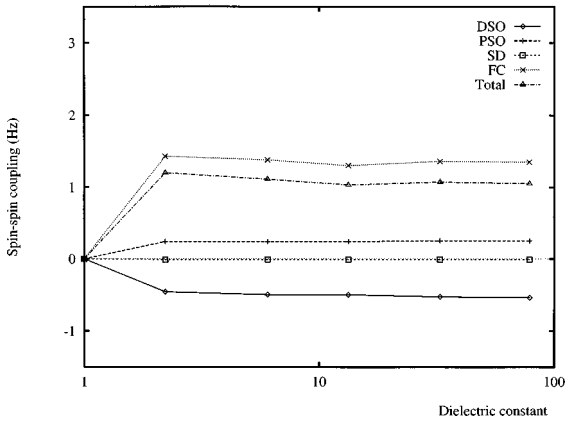

FIG. 5. Proton-proton spin–spin coupling as a function of the dielectric constant. $^2J^{HH}_{DSO}(\epsilon=1)=-1.36$ Hz, $^2J^{HH}_{PSO}(\epsilon=1)=1.27$ Hz, $^2J^{HH}_{SD}(\epsilon=1)=0.15$ Hz, $^2J^{HH}_{FC}(\epsilon=1)=-16.53$ Hz, and $^2J^{HH}(\epsilon=1)=-16.47$ Hz.

for $^1J^{SeH}$, we compare the FC term calculated for the optimized gas-phase geometry with the same constant for a geometry optimized in the dielectric continuum, see Fig. 6. The geometrical changes that occur upon solvation of the molecule change the sign of the predicted solvent shift of the coupling constant. Clearly, the subtle changes in the geometry govern the solvent shifts, which are therefore hard to model more accurately. $^2J^{HH}$ has been measured for SeHD in 30% CH_2Cl_2 at $-56°$ C to -13.5 ± 0.3 Hz.[12] We obtain a gas-phase value of -16.5 Hz and the solvent effect is ~ 1.1 Hz, in reasonable agreement with experiment. In particular, our solvent shift improves the agreement with experiment.

VII. CONCLUDING REMARKS

We have presented a method for calculating the indirect nuclear spin–spin coupling constants of a molecule embedded in a dielectric medium. The implementation has been used to calculate the dielectric effects on the nuclear shieldings and spin–spin couplings of dihydrogen selenide. Care has been taken to ensure that the calculated properties are converged with respect to the basis set and correlation treatment. It has been demonstrated that the influence of a dielectric medium may be substantial both on the nuclear shieldings and on the spin–spin couplings. It has been shown that an induced solvent shift on the spin–spin coupling constants may either be dominated by a polarization of the electronic charge distribution upon solvation, or by the geometry changes induced by solvation.

Although we have compared our results with experiment, such comparisons are difficult owing to the large temperature dependence of, for instance, the selenium shielding constant and that the experiments have been carried out in the solid state. However, our results confirm experimental findings (where these are available). For the spin–spin couplings, the introduction of a dielectric medium improves the agreement with experiment for the $^2J^{HH}$ coupling constant, whereas it gets worse in the case of $^1J^{SeH}$. However, in the latter case, this may be an artifact caused by the neglect of relativistic effects.

Note added in proof. Since the acceptance of this paper, preliminary results for the coupling constants in the hydrogen selenide molecule obtained from four-component Dirac–Fock RPA calculations have been communicated to us by Dr. Lucas Visscher. These results indicate a sizable reduction of $^1J^{HSe}$ of about 50 Hz due to relativistic effects, whereas only marginal increases in the $^2J^{HH}$ coupling due to these effects are observed. Applying these preliminary relativistic corrections to our data, our results compare very favorable with experiment.

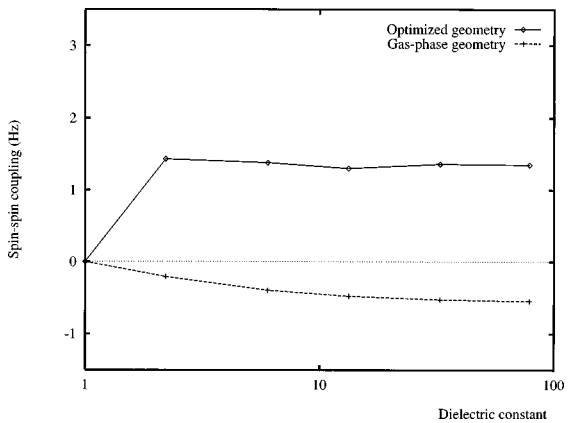

FIG. 6. Proton-proton Fermi-contact term as a function of the dielectric constant.

[1] H. J. Jakobsen, A. J. Zozulin, P. D. Ellis, and J. D. Odom, J. Magn. Reson. **38**, 219 (1980).
[2] G. Facey, R. E. Wasylishen, M. J. Collins, C. I. Ratclifle, and J. A. Ripmcester, J. Phys. Chem. **90**, 2047 (1986).
[3] P. D. Ellis, J. D. Odom, A. S. Lipton, Q. Chen, and J. M. Gulick, in *Nuclear Magnelic Shieldings and Molecular Structure*, Vol. 386 of *NATO ASI Series C*, edited by J. Tossell (Kluwer, Dordrecht, 1993), pp. 539–555.
[4] Organic Selenium Compounds, *Their Chemistry and Biology*, edited by D. L. Klayman and W. H. H. Gunther (Wiley, New York, 1973).
[5] *Selenium*, edited by R. A. Zingaro and W. C. Cooper (Van Nostrand-Reinhold, New York, 1974).
[6] C. Paulmier, *Selenium Reagents and Intermediates in Organic Synthesis* (Pergamon Oxford, 1986).
[7] A. Krief and L. Hevesi, *Organoselenium Chemistry* (Springer Verlag, Berlin, 1988).
[8] C. Brevard and P. Granger, *Handbook of High Resolution Multinuclear NMR* (Wiley, New York, 1981).
[9] *Mullinuclear NMR*, edited by J. Mason (Plenum, New York, 1987).
[10] H. E. Walchli, Phys. Rev. **90**, 331 (1953).
[11] T. Birchall, R. J. Gillespie, and S. L. Vekris, Can. J. Chem. **43**, 1672 (1965).
[12] G. Pfisterer and H. Dreeskamp, Ber. Bunsenges. **73**, 654 (1969).
[13] W. McFarlane and R. J. Wood, J. Chem. Soc. Dalton Trans. **1972**, 1397.
[14] J. D. Odom, W. H. Dawson, and P. D. Ellis, J. Am. Chem. Soc. **101**, 5815 (1979).
[15] J. A. Tossel and P. Lazzcretti, J. Magn. Reson. **80**, 39 (1988).
[16] H. Nakatsuji, T. Higashioji, and M. Sugimoto, Bull. Chem. Soc. Jpn. **66**, 3235 (1993).
[17] G. Magyarfalvi and P. Pulay, Chem. Phys. Lett. **225**, 280 (1994).
[18] V. G. Malkin, O. L. Malkina, M. E. Casida, and D. Salahub, J. Am. Chem. Soc. **116**, 5898 (1994).
[19] M. Bühl, J. Gauss, and J. F. Stanton, Chem. Phys. Lett. **241**, 248 (1995).
[20] M. Bühl, W. Thiel, U. Fleischer, and W. Kutzelnigg, J. Phys. Chem. **99**, 4000 (1995).
[21] G. Schreckenbach, Y. Ruiz-Morales, and T. Ziegler, J. Chem. Phys. **104**, 8605 (1996).
[22] C. J. Jameson and A. K. Jameson, Chem. Phys. Lett. **135**, 254 (1987).
[23] *Nuclear Magnetic Shieldings and Molecular Struclure* in Vol. 386 of *NATO ASI Series C*, edited by J. A. Tossell (Kluwer, Dordrecht, 1993).

[24] M. Schindler and W. Kutzelnigg, J. Chem. Phys. **76**, 1919 (1982).
[25] K. Wolinski, J. F. Hinton, and P. Pulay, J. Am. Chem. Soc. **112**, 8251 (1990).
[26] T. Helgaker and P. Jørgensen, J. Chem. Phys. **95**, 2595 (1991).
[27] J. Gauss, Chem. Phys. Lett. **191**, 614 (1992).
[28] J. Gauss, Chem. Phys. Lett. **229**, 198 (1994).
[29] O. Vahtras, H. Ågren, P. Jørgensen, H. J. Aa. Jensen, S. B. Padkjær, and T. Helgaker, J. Chem. Phys. **96**, 6120 (1992).
[30] D. B. Chesnut and B. E. Rusiloski, J. Mol. Struct.: THEOCHEM **314**, 19 (1994).
[31] K. V. Mikkelson, P. Jørgensen, K. Rund, and T. Helgaker, J. Chem. Phys. **106**, 1170 (1997).
[32] J. F. Hinton and D. C. Bennet, Chem. Phys. Lett. **116**, 292 (1985).
[33] J. F. Hinton, P. Guthrie, P. Pulay, and K. Wolinski, J. Am. Chem. Soc. **116**, 292 (1992).
[34] V. G. Malkin, O. L. Malkina, G. Steincbrunner, and H. Huber, Chem. Eur. J. **2**, 452 (1996).
[35] K. V. Mikkelsen, K. Rund, and T. Helgaker, Chem. Phys. Lett. **253**, 443 (1996).
[36] T. M. Nymand, P.-O. Åstrand, and K. V. Mikkelsen, J. Phys. Chem. B **101**, 4105 (1997).
[37] A. D. Buckingham, T. Schaefer, and W. G. Schneider, J. Chem. Phys. **32**, 1227 (1960).
[38] N. F. Ramsey Phys. Rev. **91**, 303 (1953).
[39] D. Matsuoka and T. Aoyama, J. Chem. Phys. **73**, 5718 (1980).
[40] J. Olsen and P. Jørgensen, J. Chem. Phys. **82**, 3235 (1985).
[41] K. V. Mikkelsen, E. Dalgaard, and P. Swanstrøm, J. Phys. Chem. **91**, 3081 (1987).
[42] K. V. Mikkelsen, H. Ågren, H. J. Aa.Jensen, and T. Helgaker, J. Chem. Phys. **89**, 3086 (1988).
[43] K. V. Mikkelsen, P. Jørgensen, and H. J. Aa. Jensen, J. Chem. Phys. **100**, 6597 (1994).
[44] K. V. Mikkelsen and K. O. Sylvester-Hvid, J. Phys. Chem. **100**, 9116 (1996).
[45] K. V. Mikkelsen and P. Jørgensen (in preparation).
[46] K. Pierloot, B. Dumez, P.-O. Widmark, and B. O. Roos, Theor. Chim. Acta **90**, 87 (1995;).
[47] P.-O. Åstrand and K. V. Mikkelsen, J. Chem. Phys. **104**, 648 (1996).
[48] P.-O. Åstrand, K. V. Mikkelsen, K. Rund, and T. Helgaker, J. Phys. Chem. **100**, 19771 (1996).
[49] P.-O. Åstrand, K. Rund, K. V. Mikkelsen, and T. Helgaker (submitted).
[50] K. Rund, P.-O. Åstrand, T. Helgaker, and K. V. Mikkelsen, J. Mol. Struct.: THEOCHEM **388**, 231 (1996).
[51] J. Olsen, B. O. Roos, P. Jørgensen, and H. J. Aa. Jensen, J. Chem. Phys. **89**, 2185 (1988).
[52] P.-A. Malmqvist, A. Rendell, and B. O. Roos, J. Phys. Chem. **94**, 5477 (1990).
[53] *Landoll-Börnstein, Zahlenwerte and Funklionen, Neue Serie* (Springer, Berlin, 1987), Vol. 11/15.
[54] T. U. Helgaker, J. Almlöf, H. J. Aa. Jensen, and P. Jørgensen, J. Chem. Phys. **84**, 6266 (1986).
[55] K. V. Mikkelsen, T. Helgaker, and H. J. Aa. Jensen (in preparation).
[56] M. Jaszuński, A. Górska, T. Helgaker, and K. Rund, Theor. Chem. Acc. (to be published).
[57] O. Vahtras, H. Ågren, P. Jørgensen, T. Helgaker, and H. J. Aa. Jensen, Chem. Phys. Lett. **209**, 201 (1993).
[58] J. Geertsen, J. Oddershede, W. T. Raynes, and T. L. Marvin, Mol. Phys. **82**, 29 (1994).
[59] G. B. Bacskay, Chem. Phys. Lett. **242**, 507 (1995).
[60] F. Mauri, B. G. Pfommer, and S. G. Louie, Phys. Rev. Lett. **77**, 5300 (1996).
[61] T. M. Nymand and P.-O. Åstrand, J. Chem. Phys. **106**, 8332 (1997).
[62] S. Kirpekar, H. J. Aa. Jensen, and J. Oddershede, Theor Chim Acta **95**, 35 (1997).